

学位申請論文

①

大環状テトラアミン亜鉛錯体を用いた
リン酸エステルの加水分解
—アルカリホスファターゼにおける
亜鉛イオンとセリン残基の役割—

広島大学大学院医学系研究科分子薬学系専攻活性構造化学

指導教授 木村 榮一

児玉 頼光

論文要旨

アルカリホスファターゼ(AP)は、リン酸モノエステルの加水分解やリン酸転移反応を触媒する亜鉛酵素であり、その活性中心は2つの亜鉛イオンとそれらを固定するアミノ酸残基および亜鉛イオン近傍のセリン残基とから構成されている。現在、この酵素の反応機構として、リン酸モノエステルのリン酸がセリン残基に転移したホスホセリン中間体の存在が確認されている。この中間体の形成には、亜鉛イオンとセリン残基とから生成したアルコキシド($Zn^{II}-OR$)の関与が推察されているが明確な証拠は得られていない。また、他の多くの亜鉛酵素による加水分解反応における亜鉛イオンに配位した水酸化物イオン($Zn^{II}-OH$)による1段階反応に比べ、中間体を經由する反応機構の有利な点も得られていない。

私は、APのセリン残基や亜鉛イオンの役割および反応機構の解明を目的として、1)ベンジルアルコールをペンダントに持つサイクレンを新規合成し、2)その亜鉛錯体を単離した。亜鉛錯体は、アルコールペンダントが亜鉛イオンに配位したアルコール型錯体およびそのアルコール型錯体のアルコールからプロトンが解離したアルコキシド型錯体を各々単離した。pH滴定法により亜鉛錯体の亜鉛イオンに配位したアルコールペンダントの酸解離定数は7.51と決定され、アルコールは亜鉛イオンに配位することによって生理pH付近でアルコキシドを形成できることが示唆された。3)さらに、アルコキシド型錯体のX線結晶構造解析より、この錯体においてアルコキシドが亜鉛イオンに配位していることがわかった。4)亜鉛錯体とビス(4-ニトロフェニル)リン酸(BNP)との反応をNMRによって追跡した結果、この反応は、 $Zn^{II}-OR$ がBNPを求核攻撃することによってリン酸エステルがアルコールペンダントに転移したリン酸ジエステル中間体を形成したのち、その中間体のリン酸ジエステルペンダントが分子内 $Zn^{II}-OH$ によって加水分解され、リン酸モノエステルペンダントを持つ最終生成物が生成することがわかった。最終生成物においては、リン酸モノエステルペンダントの亜鉛イオンへの配位によって亜鉛錯体の加水分解活性が失われていた。このことから、リン酸モノエステルペンダントの加水分解には、 Zn^{II} -cyclenなどの求核体の分子内へ導入が必要であることがわかった。5)中間体は単離、同定した。6)BNPと亜鉛錯体とから中間体が生成する反応をpH6-10で検討した。得ら

れたシグモイド曲線から速度論的酸解離定数は 7.4 となり、pH 滴定法から求めた亜鉛錯体の酸解離定数 7.3 とほぼ一致した。この結果、この反応の活性種はアルコキシド型錯体であると結論された。この反応の 2 次反応速度定数は $6.5 \times 10^{-4} \text{ M}^{-1}\text{s}^{-1}$ と決定され、 Zn^{II} -methylcyclen による BNP の加水分解反応速度定数 $5.2 \times 10^{-6} \text{ M}^{-1}\text{s}^{-1}$ の 125 倍にもなり、 Zn^{II} -OR は Zn^{II} -OH よりも強い求核体であることがわかった。7) 中間体から最終生成物へのリン酸ジエステルペンダント加水分解反応を pH 6-10 で検討した。得られたシグモイド曲線から速度論的酸解離定数は 9.0 となり、pH 滴定法から求めた中間体の亜鉛イオンの配位水の酸解離定数 9.1 とほぼ一致した。この結果、この反応の活性種は分子内 Zn^{II} -OH であると結論された。この反応の 1 次反応速度定数は $3.5 \times 10^{-5} \text{ s}^{-1}$ と決定した。8) 同様の加水分解反応が分子間で起きた場合のモデルとして Zn^{II} -methylcyclen と 4-ニトロフェニル エチル リン酸との反応 (2 次反応速度定数: $7.9 \times 10^{-7} \text{ M}^{-1}\text{s}^{-1}$) を考えると、速度定数の比較から、リン酸ジエステルと亜鉛錯体との分子間反応が分子内で起きることによる有効モル濃度は 45 M となった。この結果、基質を求核体の非常に近い位置に固定することによって反応性が上がるということがわかった。

これら新規亜鉛錯体を用いた実験から、AP の反応機構において、1) Zn^{II} -OR は生理 pH の水溶液中で容易に生成すること、2) Zn^{II} -OR は Zn^{II} -OH よりも求核性が強く、リン酸転移反応が容易に起きること、3) ホスホセリン中間体は、亜鉛イオン近傍にあり、 Zn^{II} -OH による加水分解の反応性が高いこと、4) リン酸モノエステルと亜鉛錯体とは 1 : 1 の複合体を形成するため、リン酸モノエステルの加水分解には 2 分子の亜鉛錯体が必要であることがわかった。このモデル化学的反應の検討により生体機能の解明に大きく貢献できたと考える。

Contents

	page
Abstract	1
1. Introduction	2
2. Results and Discussion	
2-1. Synthesis of Benzyl Alcohol-Pendant Cyclen	5
2-2. Protonation and Zinc(II) Complexation Constants of the Benzyl Alcohol-Pendant Cyclen	5
2-3. X-ray Crystal Structure of the Zn ^{II} Complex of the Deprotonated Benzyl Alcohol-Pendant Cyclen	7
2-4. Net Reaction of the Benzyl Alcohol-Pendant Cyclen-Zn ^{II} Complex with Bis(4-nitrophenyl) Phosphate	10
2-5. A Kinetic Study of the Initial Reaction	12
2-6. Isolation of the Phosphoryl Intermediate	14
2-7. Spontaneous Hydrolysis of the Pendant Phosphodiester in the Phosphoryl Intermediate to a Phosphomonoester by the Intramolecular Zn ^{II} -OH ⁻	14
2-8. Hydrolysis of Ethyl (4-Nitrophenyl) Phosphate with an Intermolecular Nucleophile Zn ^{II} -OH ⁻	16
3. Summary and Conclusions	17
4. Experimental Section	18
References and Notes	23
Acknowledgement	25

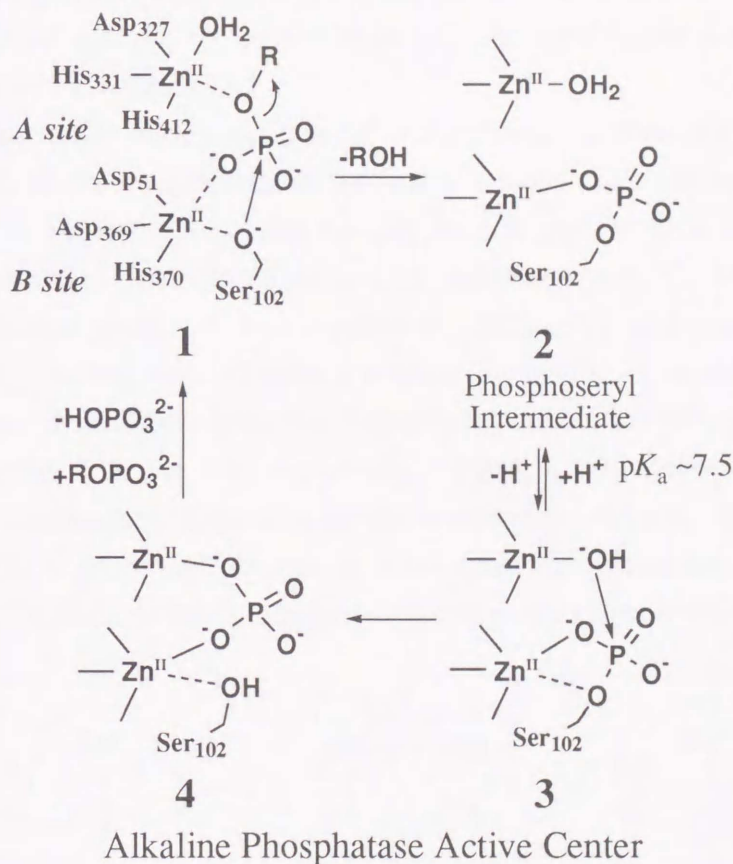
Phosphodiester Hydrolysis by a New Zinc(II) Macrocyclic Tetraamine Complex with an Alcohol Pendant: Elucidation of the Roles of Ser-102 and Zinc(II) in Alkaline Phosphatase

Abstract: A new benzyl alcohol-pendant cyclen (cyclen = 1,4,7,10-tetraazacyclododecane) ligand, (S)-1-(2-hydroxy-2-phenylethyl)-1,4,7,10-tetraazacyclododecane (L) has been synthesized. The complexation of L with Zn^{II} yielded 1:1 five-coordinate complexes (isolated as its perchlorate salts with the pendant alcohol either undissociated (ZnL) or dissociated ($ZnH_{1.1}L$) from acidic (pH 6.0) or basic (pH 9.5) aqueous solution, respectively). The pK_a value for the pendant alcohol ($ZnL \rightleftharpoons ZnH_{1.1}L + H^+$) was determined by potentiometric pH titration to be 7.30 ± 0.02 at $35^\circ C$ with $I = 0.10$ ($NaNO_3$). The X-ray crystal study of $ZnH_{1.1}L$ has shown two crystallographically distinct structures with the alkoxide closely coordinated at the fifth coordination site, where an average distance of $Zn-O$ is 1.91 \AA . The Zn^{II} -bound alkoxide anion in $ZnH_{1.1}L$ is a more reactive nucleophile than *N*-methylcyclen- Zn^{II} - OH^- species (Zn^{II} -Me-cyclen). In the kinetic study using ZnL in aqueous solution (pH 6.0–10.3) at $35^\circ C$ with $I = 0.10$ ($NaNO_3$), the rate-pH profile for a phosphoryl transfer reaction from bis(4-nitrophenyl)phosphate (BNP^-) to $ZnH_{1.1}L$ gave a sigmoidal curve with an inflection point at pH 7.4, which corresponds to the pK_a value for $ZnL \rightleftharpoons ZnH_{1.1}L + H^+$. The second-order rate constant k_{BNP} of $(6.5 \pm 0.1) \times 10^{-1} \text{ M}^{-1} \text{ s}^{-1}$ is 125 times greater than the corresponding value of $(5.2 \pm 0.2) \times 10^{-6} \text{ M}^{-1} \text{ s}^{-1}$ for BNP^- hydrolysis catalyzed by Zn^{II} -Me-cyclen. The product of the phosphoryl transfer reaction from BNP^- to $ZnH_{1.1}L$ is the pendant alcohol-phosphorylated $ZnH_{1.1}L-NPP$, which was isolated as its perchlorate salts $ZnL-NPP$ by reacting $ZnH_{1.1}L$ with BNP^- in DMF. In anhydrous DMF solution, the phosphoryl transfer (k_{BNP} of $1.1 \pm 0.1 \text{ M}^{-1} \text{ s}^{-1}$ at $35^\circ C$) is 1700 times faster than that in aqueous solution. In the subsequent reaction of $ZnL-NPP$, the pendant phosphodiester undergoes an intramolecular nucleophilic attack by the Zn^{II} -bound OH^- of $ZnH_{1.1}L-NPP$ to yield a phosphomonoester product $ZnL-P$. From the sigmoidal rate-pH relationship (pH 7.4–10.5), the kinetic pK_a value of 9.0 was estimated for $ZnL-NPP \rightleftharpoons ZnH_{1.1}L-NPP + H^+$, which is almost the same value ($pK_a = 9.10 \pm 0.05$) determined by potentiometric pH titration at $35^\circ C$. The first-order rate constant for the reaction $ZnH_{1.1}L-NPP \rightarrow ZnL-P$ is $(3.5 \pm 0.1) \times 10^{-5} \text{ s}^{-1}$ at $35^\circ C$ with $I = 0.10$ ($NaNO_3$). As a reference to this intramolecular phosphodiester hydrolysis, ethyl (4-nitrophenyl) phosphate (NEP^-) was hydrolyzed by Zn^{II} -Me-cyclen. The second-order rate constant k_{NEP} was $(7.9 \pm 0.3) \times 10^{-7} \text{ M}^{-1} \text{ s}^{-1}$ at $35^\circ C$ with $I = 0.10$ ($NaNO_3$). Thus, the intramolecular hydrolysis is 45 000 times faster than the intermolecular NEP^- hydrolysis with 1 mM Zn^{II} -Me-cyclen. The present findings that demonstrate the potential of the proximate alcohol by Zn^{II} in the initial phosphoryl transfer and the potential of the Zn^{II} -bound water in the intramolecular phosphate hydrolysis may well serve to elucidate the collaborative functions of Ser-102 and Zn^{II} ions in alkaline phosphatase.

1. Introduction

Alkaline phosphatase (AP) is a Zn^{II} -containing enzyme that nonspecifically hydrolyzes phosphate monoesters ($ROPO_3^{2-}$) at alkaline pH.¹ Intensive studies have been done on *E. coli* alkaline phosphatase. On the basis of X-ray structure² and NMR study³ of native and metallo-substituted AP, it is now accepted that, at the AP active center consisting of two Zn^{II} ions (ca. 4 Å separation), a substrate monophosphate is initially attacked by Ser-102 in **1** to yield a phosphoseryl-enzyme intermediate **2**, which subsequently is attacked by the adjacent Zn^{II} -OH⁻ to complete the hydrolysis **3** → **4** and reproduce the free form of serine to reinitiate the catalytic cycle (see Scheme 1).⁴

Scheme 1

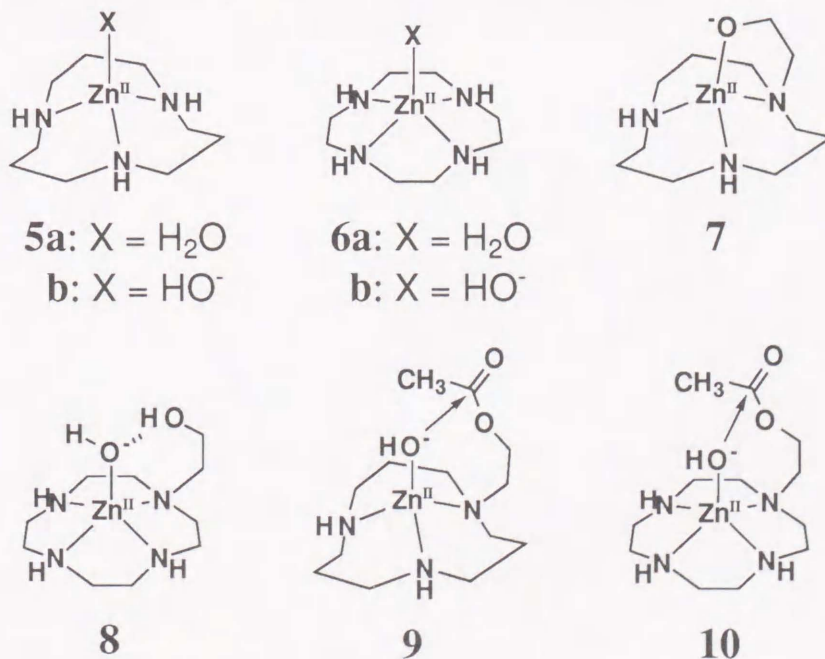


In Scheme 1, the A-site Zn^{II} serves to coordinate the phosphate substrate to make it vulnerable to the attack of Ser-102 that is potentiated by the B site Zn^{II} (**1**). After the phosphate is transferred from the substrate to Ser(102) (**2**), the vacated coordination site of the A-site Zn^{II} activates an H_2O as Zn^{II} -OH⁻, which becomes an intramolecular nucleophile in the final dephosphorylation (**3** → **4**). The wild-type AP reaches maximal activity around pH 8, where the rate-limiting step is release of the tightly bound inorganic phosphate (the product) from the enzyme-product complex **4**. Accordingly, inorganic phosphate is a competitive inhibitor. At pH < 5.5, the phosphoseryl intermediate (**2**) is stable.^{3d,5}

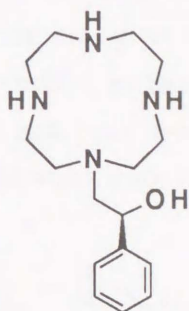
There are some intrinsic questions concerning the AP mechanism, such as (i) what is the special advantage in forming the phosphoseryl intermediate **2** for indirect hydrolysis and (ii) how does the Ser-102 associated with the Zn^{II} ion become a nucleophile? Recently, the Ser-102 in AP was replaced using site-directed mutagenesis by Leu or Ala.⁶ The mutant enzymes still catalyzed the phosphate hydrolysis, with similar rate-pH profiles, although the catalytic efficiency is 1/500 to 1/1000 of that of the wild-type enzyme, for which the direct hydrolysis of the substrate by $Zn^{II}-OH^-$ was proposed. In other hydrolytic metalloenzymes, the direct hydrolysis by $M-OH^-$ species seems more prevalent.⁷

There have been numerous studies of phosphatase model systems using simple metal complexes,^{8,9} but most of these models have been built for *the sole $M-OH^-$ systems as nucleophiles, while few were concerned with the net reaction initiated by the metal-bound alcohol, followed by the metal-bound water, as was revealed by AP.*

Recently, our laboratory discovered that Zn^{II} -1,5,9-triazacyclododecane ([12]aneN₃) complex **5a**^{10,11} and Zn^{II} -1,4,7,10-tetraazacyclododecane (cyclen) complex **6a**¹² can activate an H₂O as the Zn^{II} -bound OH⁻ species **5b** ($pK_a = 7.3$) and **6b** ($pK_a = 7.9$) and that both catalyze hydrolysis of carboxyesters,^{10a-c} β -lactams,¹² phosphotriesters, and phosphodiester.^{10c} Our laboratory further disclosed that the alcohol-pendant *N*-hydroxyethyl on [12]aneN₃ and cyclen formed 1:1 Zn^{II} complexes **7**¹³ and **8**,¹⁴ which more efficiently catalyze 4-nitrophenyl acetate hydrolysis. These were the novel models of metalocatalysts that *indirectly* hydrolyze the carboxyl ester via the rate-limiting "acyl intermediates" **9** and **10**, respectively. Using **8** and bis(4-nitrophenyl) phosphate (BNP⁻), we also had checked the phosphatase activity in aqueous solution. The phosphoryl transfer reaction from BNP⁻ to **8** could be followed as 4-nitrophenolate production,¹⁵ but the following reaction was too complex to allow the elucidation of the total reaction mechanism.



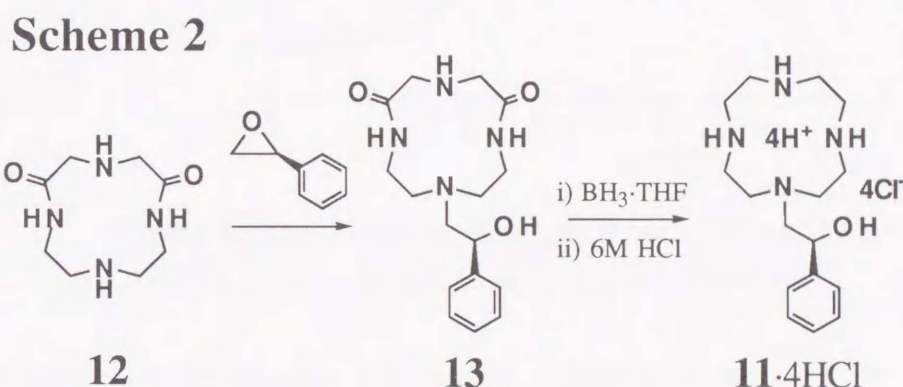
In this study, I synthesized a new benzyl alcohol-pendant cyclen **11**, bearing a chiral carbon adjacent to the phenyl group. I have discovered that **11** yields a 1:1 Zn^{II} complex whose phosphoester bond cleavage activity has a very distinct reaction mechanism. I herein describe a novel chemical model for Zn^{II} -involving serine enzymes as part of our series of studies on the intrinsic chemical properties of Zn^{II} in alkaline phosphatase.



11

2. Results and Discussion

2-1. Synthesis of (*S*)-1-(2-Hydroxy-2-phenylethyl)-1,4,7,10-tetraazacyclododecane (Benzyl Alcohol-Pendant Cyclen, **11) (Scheme 2).** The macrocyclic dioxotetraamine **12**¹⁶ and (*S*)-styrene oxide were heated to reflux in EtOH for 1 day to obtain (*S*)-1-(2-hydroxy-2-phenylethyl)-5,9-dioxo-1,4,7,10-tetraazacyclododecane **13** in 46% yield. Both amide groups were reduced with BH₃-THF complex in THF to give (*S*)-1-(2-hydroxy-2-phenylethyl)-1,4,7,10-tetraazacyclododecane (**11**), which was isolated as its tetrahydrochloride salt from 6 M HCl aqueous solution in 62% yield. Using *rac*-styrene oxide as the starting material, the corresponding racemic ligand was yielded in 24%. For all the following studies, we used the enantiomeric product **11**.



2-2. Protonation and Zinc(II) Complexation Constants of the Benzyl Alcohol-Pendant Cyclen (11**).** The protonation constants (K_a) of **11** were determined by potentiometric pH titrations of **11**·4HCl (1 mM) using 0.10 M NaOH with $I = 0.10$ (NaClO₄) at 25 °C. A typical pH titration curve is shown in Figure 1a. The titration data were analyzed for equilibria 1–4. The mixed protonation constants K_1 – K_4 (a_{H^+} is the activity of H⁺) are defined as follows:

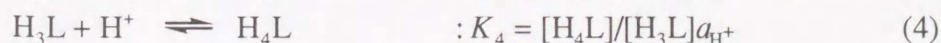
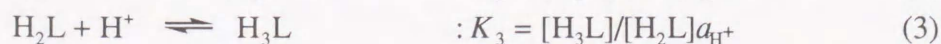
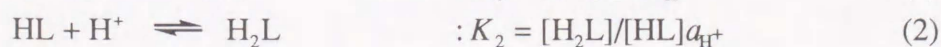
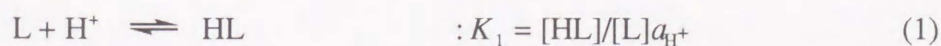


Table 1 summarizes the obtained protonation constants ($\log K_n$) in comparison with the reported K_n values of cyclen and *N*-(hydroxyethyl)cyclen (HE-cyclen) under the same conditions. The K_1 and K_2 values of **11** are extremely large with respect to K_3 and K_4 values, which are roughly the same as those of cyclen and HE-cyclen.

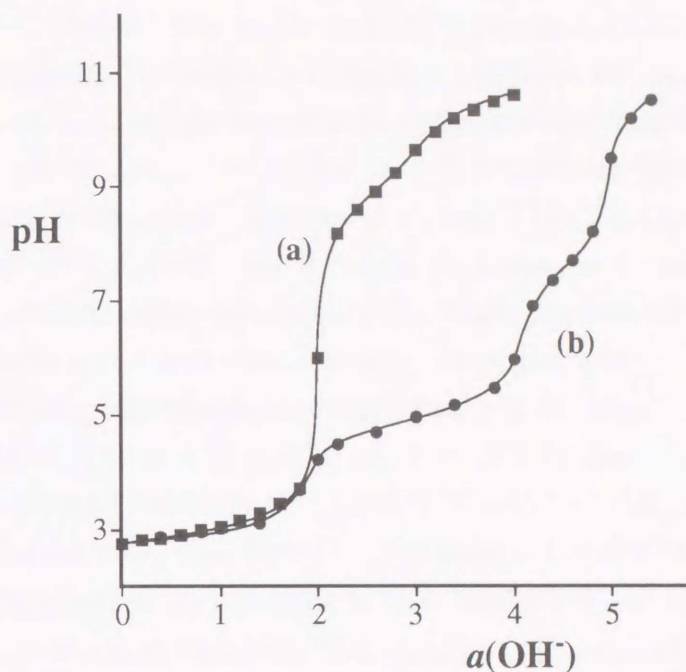


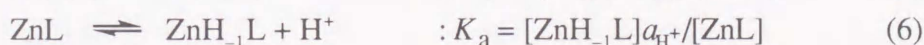
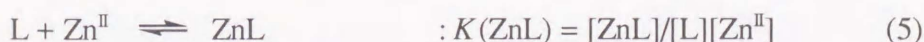
Figure 1. Typical titration curves for **11** at 25 °C with $I = 0.10$ (NaClO_4): (a) 1.0 mM of **11**·4HCl; (b) a + 1.0 mM ZnSO_4 .

Table 1. Comparison of the Protonation Constants of Cyclen Ligands and Zn^{II} Complexation Constants ^(a)

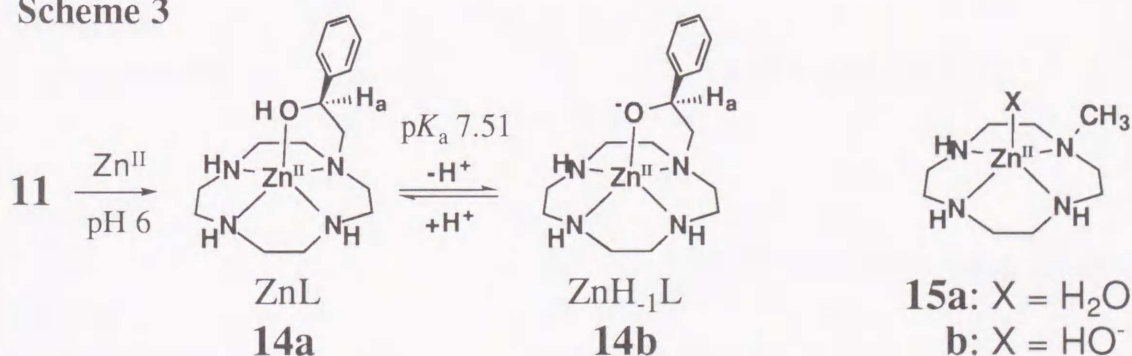
	11	cyclen	HE-cyclen	methylcyclen
$\log K_1$	10.92 ± 0.05 ^(b)	11.04 ^(f)	10.72 ^(f)	
$\log K_2$	8.87 ± 0.03 ^(b)	9.86 ^(f)	9.28 ^(f)	
$\log K_3$	< 2 ^(b)	< 2 ^(f)	< 2 ^(f)	
$\log K_4$	< 2 ^(b)	< 2 ^(f)	< 2 ^(f)	
$\log K(\text{ZnL})$	13.6 ± 0.1 ^(c)	15.3 ^(f)	13.8 ^(f)	15.1 ⁽ⁱ⁾
$\text{p}K_a$ 25 °C	7.51 ± 0.02 ^(d)	7.86 ^(g)	7.60 ^(h)	7.68 ⁽ⁱ⁾
35 °C	7.30 ± 0.02 ^(e)	7.64 ^(g)	7.41 ^(h)	7.50 ± 0.02 ⁽ⁱ⁾

^(a) $K_n = [\text{H}_n\text{L}]/[\text{H}_{n-1}\text{L}]a_{\text{H}^+}$. $K(\text{ZnL}) = [\text{ZnL}]/[\text{L}][\text{Zn}^{\text{II}}]$. $\text{p}K_a = -\log([\text{ZnH}_1\text{L}]/[\text{ZnL}])$. ^(b) At 25 °C with $I = 0.10$ (NaClO_4). ^(c) Determined with 1.0 mM of **14a** and 4 equiv amount of HClO_4 at 25 °C with $I = 0.10$ (NaClO_4). ^(d) Determined with 1.0 mM of **14a** and $I = 0.10$ (NaClO_4). ^(e) Determined with 1.0 mM of **14a** and $I = 0.10$ (NaNO_3). ^(f) From ref 14 at 25 °C with $I = 0.10$ (NaClO_4). ^(g) From ref 12 with $I = 0.10$ (NaClO_4). ^(h) From ref 14 with $I = 0.10$ (NaClO_4). ⁽ⁱ⁾ From ref 17 at 25 °C with $I = 0.10$ (NaClO_4). ^(j) Determined with 1.0 mM of **15a** and $I = 0.10$ (NaNO_3)

The potentiometric pH titration curve of **11**·4HCl in the presence of an equimolar amount of Zn^{II} using 0.10 M NaOH (Figure 1b) revealed two distinct equilibria: the first is the ZnL complex formation at 4 < pH < 6 until *a* = 4, and the second is monodeprotonation from ZnL (4 < *a* < 5). Up to *a* = 4, the equilibration was extremely slow, so that we had to wait more than 2 h for each titration point. The titration data were treated for the 1:1 ZnL (**14a**) complex (eq 5) and its monodeprotonated complex ZnH₋₁L (**14b**) (eq 6), where H₋₁L denotes alcoholic OH-deprotonated ligand (Scheme 3). The obtained values log *K*(ZnL) at 25 °C and deprotonation constants p*K*_a at 25 and 35 °C are listed in Table 1. Any further deprotonation or precipitation of Zn(OH)₂ was not observed over pH 12, indicating the monodeprotonated species to be stable until pH ca. 12. The deprotonation constants p*K*_a (eq 6) of 7.51 ± 0.02 and 7.30 ± 0.02 determined by the pH-metric titration respectively at 25 °C with *I* = 0.10 (NaClO₄) and 35 °C with *I* = 0.10 (NaNO₃) are near those of **6a**¹² and Zn^{II}-*N*-methylcyclen **15a**¹⁷ (see Table 1). Fortunately, both the ZnL (**14a**) and ZnH₋₁L (**14b**) complexes were crystallized as their perchlorate salts from pH 6 and 9.5 aqueous solutions, respectively. The structure of the monodeprotonated complex **14b** was confirmed by the X-ray crystal analysis (vide infra). As the solution pH became higher, the chemical shifts of the benzyl proton H_a for **14** moved upfield from δ 5.14 at pD 6.0 (**14a**) to δ 4.86 at pD > 9.5 (**14b**). From these facts and the following results, we assigned the deprotonated structure to be **14b** rather than Zn^{II}-OH⁻ species in aqueous alkaline solution.



Scheme 3



2-3. X-ray Crystal Structure of the Zn^{II} Complex of the Deprotonated Benzyl Alcohol-Pendant Cyclen (**14b**). When the benzyl alcohol-pendant cyclen **11** (in the acid-free form L, see the Experimental Section) in water was mixed with 1 equiv of Zn^{II}(ClO₄)₂·6H₂O at 60 °C, **14a**·(ClO₄)₂ was obtained as colorless crystals. Addition of 1 equiv of NaOMe to **14a**·(ClO₄)₂ in MeOH gave **14b**·ClO₄, which was recrystallized from aqueous alkaline solution (pH 9.5).

Figure 2 shows an ORTEP drawing of **14b**·ClO₄ with 30% probability thermal ellipsoids. Selected crystal data and collection parameters are displayed in Table 2. In this Zn^{II} complex, there are two crystallographically distinct molecules (Figure 2a,b). The Zn^{II} ions Zn₁ and Zn₂, respectively, lie above the four nitrogen atoms (N₁, N₄, N₇, N₁₀ and N₂₂, N₂₅, N₂₈, N₃₁), and are apically bound with the pendant alkoxide oxygens O₁₅ and O₃₆, respectively. The angles N₁–Zn₁–N₇ and N₂₂–Zn₂–N₂₈ and N₄–Zn₁–N₁₀ and N₂₅–Zn₂–N₃₁ are respectively bent at (138.5 and 139.2°) and (135.0 and 134.5°) indicating distorted tetragonal-pyramidal structures. The average Zn–O bond distance of 1.91 Å is much shorter than the Zn–N bonds (2.056–2.173 Å). The Zn–O distance is shorter in the Zn^{II}–anion donor than in other Zn^{II}–macrocyclic polyamine complexes.^{10b,13,14,18} The earlier Zn–O bond distance with the neutral alcohol pendant in **8** was 1.994 Å.¹⁴ The apical Zn–O bond is bent with the N₁–Zn₁–O₁₅ and N₂₂–Zn₂–O₃₆ angles of 86.8 and 86.7°, respectively. One may view **14b** as having a distorted trigonal-bipyramidal structure with N₁, N₇, and O₁₅ as equatorial donors and N₄ and N₁₀ as axial donors.

Although the pendant alkoxide donor binds firmly with Zn^{II} in the solid state, this bonding would be kinetically labile in DMF and H₂O solutions, so that this alkoxide anion can be a good nucleophile for the phosphoryl transfer reaction with BNP⁻.

Table 2. Selected Crystallographic Data for **14b**·ClO₄.

empirical formula (formula weight)	C ₁₆ H ₂₇ N ₄ O ₅ ClZn (456.25)
crystal color, habit	colorless, prismatic
crystal system	orthorhombic
space group	<i>P</i> 2 ₁ 2 ₁ 2 ₁ (no. 19)
lattice parameters	<i>a</i> = 16.977(4), <i>b</i> = 18.135(4), <i>c</i> = 13.173(3) Å <i>V</i> = 4055(1) Å ³ <i>Z</i> = 8
μ (Cu K α)	31.96 cm ⁻¹
radiation	Cu K α (λ = 1.541 78 Å), graphite monochromated
scan type	ω -2 θ
scan rate (in ω)	16.0 deg/min (five scans)
scan width	(1.42 + 0.30 tan θ)°
2 θ _{max}	120.2°
no. of reflsn measd	3414 (total)
refinement	full-matrix least squares
no. of obs (<i>I</i> > 3.00 σ (<i>I</i>))	2862
residuals: <i>R</i> ; <i>R</i> _w	0.050; 0.077

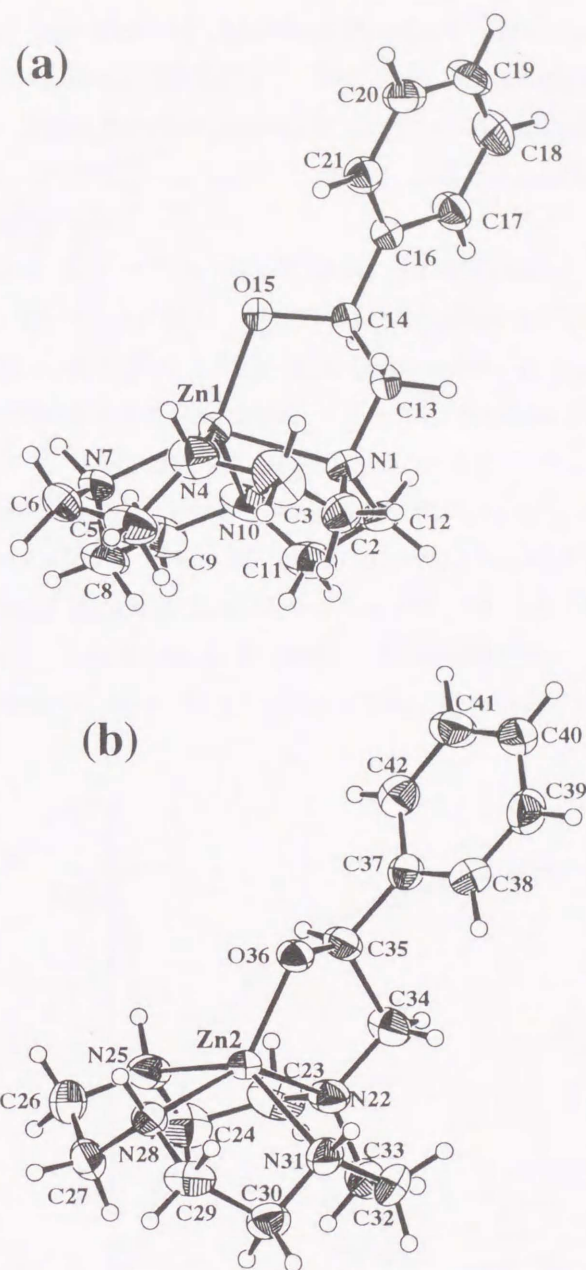


Figure 2. ORTEP drawing (30% probability ellipsoids) of the two crystallographically distinct molecules (a and b) of **14b**·ClO₄. ClO₄ anions were omitted for clarity.

Bond distances: (a) Zn(1)–O(15) 1.915(5), Zn(1)–N(1) 2.172(7), Zn(1)–N(4) 2.173(8), Zn(1)–N(7) 2.067(7), Zn(1)–N(10) 2.143(8) Å; (b) Zn(2)–N(22) 2.155(7), Zn(2)–N(25) 2.161(8), Zn(2)–N(28) 2.056(7), Zn(2)–N(31) 2.169(7) Å. Bond angles: (a) N(1)–Zn(1)–N(4) 81.2(3), N(1)–Zn(1)–N(7) 81.4(4), N(4)–Zn(1)–N(7) 84.0(4), N(7)–Zn(1)–N(10) 82.2(4), O(15)–Zn(1)–N(1) 86.8(2)°; (b) N(22)–Zn(2)–N(25) 82.8(4), N(22)–Zn(2)–N(31) 80.6(3), N(25)–Zn(2)–N(28) 82.1(3), N(28)–Zn(2)–N(31) 82.8(3), O(36)–Zn(2)–N(22) 86.7(2)°.

2-4. Net Reaction of the Benzyl Alcohol-Pendant Cyclen-Zn^{II} Complex 14b with Bis(4-nitrophenyl) Phosphate (BNP⁻). The ZnH₁L complex **14b** has been tested as a simplified model of AP. Since the phosphomonoester (e.g., 4-nitrophenyl phosphate (NPP²⁻)) was hydrolyzed impractically slowly, we used a more reactive substrate, phosphodiester bis(4-nitrophenyl) phosphate (BNP⁻).

The overall reaction of BNP⁻ (25 mM) with **14b** (20 mM) was followed by the ¹H NMR of the benzyl protons in D₂O at 35 °C and pD = 10.3 (0.1 M CHES buffer) (see Figure 3). The initial product **16** (a new triplet at δ 5.56), which later was proven to be the phosphoryl intermediate, increased as the starting **14b** (δ 4.83) decreased. The final product **17** (δ 5.90, see blow) appeared subsequently. After 192 h, **14b** and **16** diminished to 2.5% and 7.5%, respectively, and the majority (90%) of the initial Zn^{II} complex was converted to **17**, where almost 2 equiv of 4-nitrophenolate was released (191% based on initial concentration of **14b**). The same reaction was followed by ³¹P NMR under the same conditions, and the products **16** and **17** were identified at δ -5.7 and 5.9, respectively. No other side product was detected. We assigned the net reaction scheme as depicted in Scheme 4, with the aid of the following results.

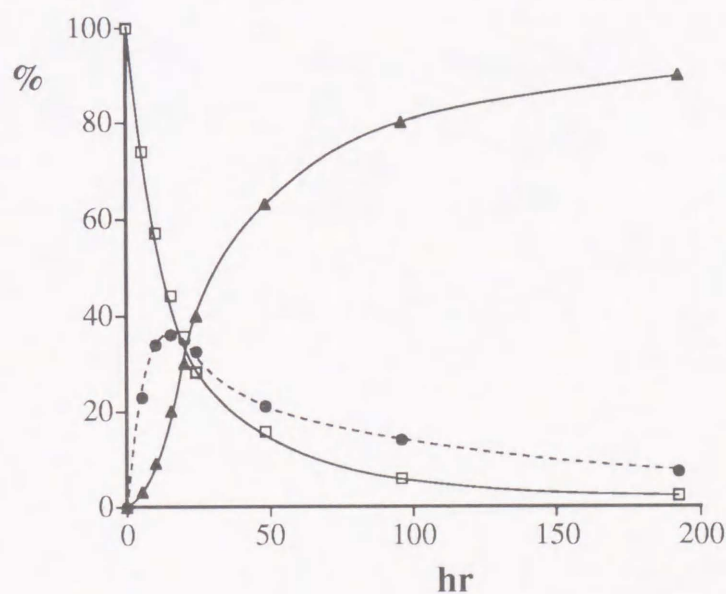
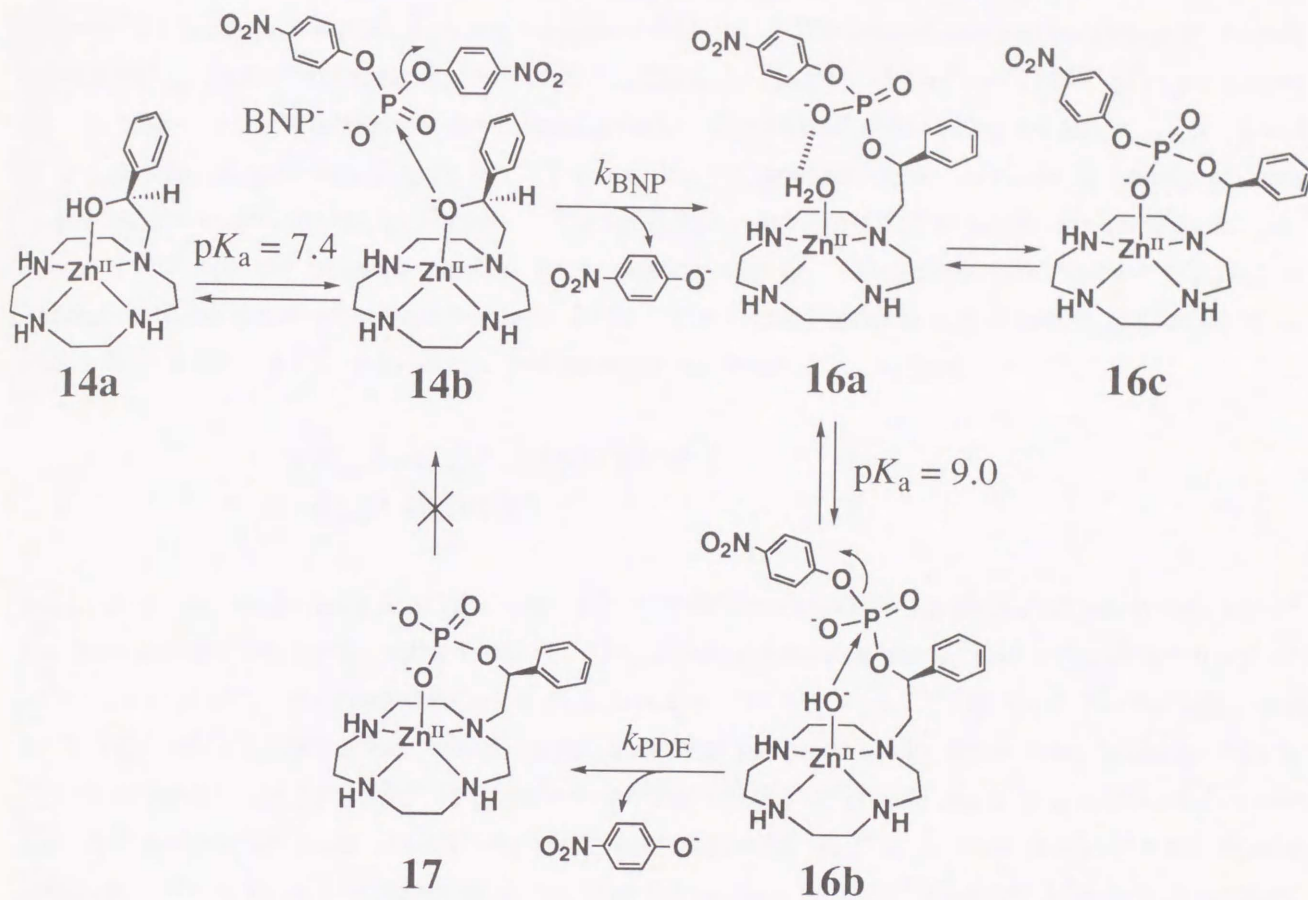


Figure 3. Time course of the relative concentrations of Zn^{II} complexes **14b** (open square), **16** (solid circle), and **17** (solid triangle) for the reaction of BNP⁻ (25 mM) with **14b** (20 mM) in D₂O at 35 °C, *I* = 0.10 (NaNO₃), and pD = 10.3 (0.1 M CHES buffer). The relative concentrations (%) are based on the initial concentration of **14b**.

Scheme 4



2-5. A Kinetic Study of the Initial Reaction 14b → 16. The initial phosphorylation rate in aqueous solution at 35 °C, $I = 0.10$ (NaNO_3), and pH 6.0–10.3 (20 mM Good's buffer) was followed by the appearance of 4-nitrophenolate at 400 nm. The second-order dependence of the rate constant k'_{BNP} on the total concentration of Zn^{II} complex ($= [14\text{a}] + [14\text{b}]$) and $[\text{BNP}^-]$ fits the kinetic eq 7, where v is the 4-nitrophenolate releasing rate. The second-order rate constant, k'_{BNP} is plotted as a function of pH (see Figure 4). The resulting sigmoidal curve indicates a kinetic process controlled by an acid–base equilibrium. The inflection point at pH 7.4 is almost the same as the $\text{p}K_{\text{a}}$ value of **14** for the pendant alcohol deprotonation (eq 6). Therefore, the reactive species is concluded to be the deprotonated complex **14b**. The second-order rate constant k_{BNP} (see eq 8) of $(6.5 \pm 0.1) \times 10^{-4} \text{ M}^{-1} \text{ s}^{-1}$ was determined from the maximum k'_{BNP} values.

$$v = k'_{\text{BNP}}[\text{total Zn}^{\text{II}} \text{ complex}][\text{BNP}^-] \quad (7)$$

$$= k_{\text{BNP}}[14\text{b}][\text{BNP}^-] \quad (8)$$

For a reference, the hydrolysis of the same substrate BNP^- (to NPP^{2-}) with Zn^{II} -*N*-methylcyclen **15** has been determined by the same method. The kinetics followed the second-order dependence on $[\text{BNP}^-]$ and **15b**. The rate constant is $(5.2 \pm 0.2) \times 10^{-6} \text{ M}^{-1} \text{ s}^{-1}$ at 35 °C, $I = 0.10$ (NaNO_3), and pH 9.3 (20 mM CHES buffer), which demonstrates that *the nucleophilic reaction catalyzed by 14b is 125 times faster than by 15b*. It is understood that *the Zn^{II} -alkoxide anion is a better nucleophile than Zn^{II} -hydroxide anion toward the phosphate substrate*, just as toward 4-nitrophenyl acetate substrate.^{13,14} It should be noted, however, that the reaction with Zn^{II} -alkoxide **14b** is a phosphoryl transfer to form a phosphoryl intermediate **16b** (see Scheme 4), as the previously found acyl transfer with **7** and **8**.^{13,14} On the other hand, the reaction with **15b** is a hydrolysis that yields NPP^{2-} .

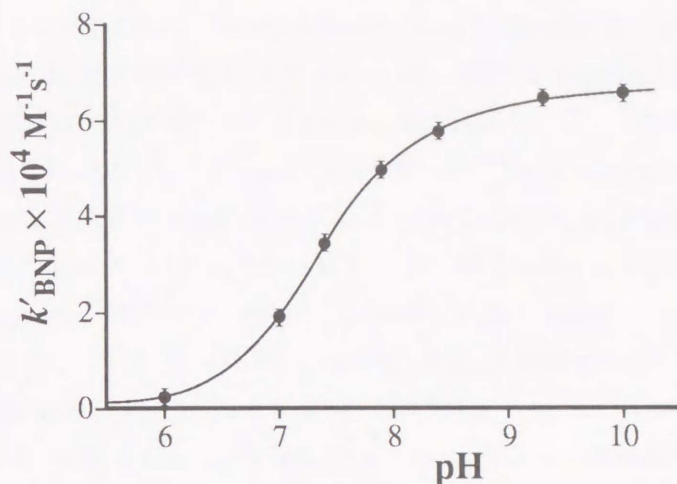


Figure 4. Rate-pH profile for the second-order rate constants of the phosphoryl transfer from BNP^- to **14** (see eq 7) at 35 °C with $I = 0.10$ (NaNO_3) in aqueous solution.

Table 3. Comparison of the Phosphodiester Bond Cleavage Rate Constants, k_{BNP} ($\text{M}^{-1} \text{s}^{-1}$), for **14b**, **8**, **15b**, **5b**, and **6b**, and Aqueous OH^- Ion in Aqueous Solution

catalyst	k_{BNP}	catalyst	k_{BNP}
14b	$(6.5 \pm 0.1) \times 10^{-4}$ (a)	5b	8.5×10^{-5} (d)
8	5.0×10^{-4} (b)	6b	2.1×10^{-5} (d)
15b	$(5.2 \pm 0.2) \times 10^{-6}$ (c)	OH^-_{aq}	2.4×10^{-5} (d)

(a) Determined with 2.0, 1.0, and 0.5 mM of **14b** and 10, 5.0, and 2.5 mM of BNP^- at 35 °C with $I = 0.10$ (NaNO_3). (b) From ref 15 at 35 °C with $I = 0.10$ (NaNO_3). (c) Determined with 16, 8.0, and 4.0 mM **14b** and 10, 5.0, and 2.5 mM BNP^- at 35 °C with $I = 0.10$ (NaNO_3). (d) From ref 10c at 35 °C with $I = 0.20$ (NaClO_4).

2-6. Isolation of the Phosphoryl Intermediate 16a from the BNP⁻ Reaction with 14b in DMF. The phosphoryl intermediate **16a** was unequivocally determined by independent isolation of **16a**·ClO₄ by the reaction of BNP⁻ and **14b** in dry DMF. The structure was identified by elemental analysis (C, H, N) and ¹H, ¹³C, and ³¹P NMR. The pH-metric titration of **16a** at 35 °C with *I* = 0.10 (NaNO₃) using 0.1 M aqueous NaOH¹⁹ showed the monodeprotonation and its p*K*_a of 9.10 ± 0.05, which is assigned to **16a** ⇌ **16b**. The p*K*_a value is higher than 7.50 ± 0.02 for **15a** ⇌ **15b** at the same conditions, which is possibly due to the proximate phosphate anion binding to the Zn^{II}, see **16c**. The ³¹P NMR chemical shift of phosphoryl intermediate **16** in H₂O changed from δ -3.6 at pD 6.5 (**16a**) to δ -6.5 at pD 11 (**16b**).

The reaction of BNP⁻ with **14b** (the isolated monoperochlorate salt was used) in dry DMF at 35 °C was kinetically studied by observing the appearance of 4-nitrophenolate at 430 nm. The second-order rate constant *k*_{BNP} (= 1.1 ± 0.1 M⁻¹ s⁻¹) with respect to [BNP⁻] and [**14b**] was obtained. The comparison of the rate constants *k*_{BNP} in DMF and aqueous solution points out that the Zn^{II}-bound alkoxide nucleophile acts 1700 times more efficiently in this aprotic solvent than in aqueous solution, which is accounted for by less interfering solvations in DMF.²⁰ This observation suggests that in hydrophobic environments a phosphoryl transfer at the enzyme active center might occur quite effectively.

2-7. Spontaneous Hydrolysis of the Pendant Phosphodiester in 16b to a Phosphomonoester 17 by the Intramolecular Zn^{II}-OH⁻. The pendant phosphodiester in **16**, the initial phosphorylation product resulting from the phosphotransfer reaction, was found to undergo spontaneous hydrolysis in alkaline aqueous solution to yield a phosphomonoester **17** (see Scheme 4). We failed to isolate **17** as a solid. This reaction was followed by the ¹H and ³¹P NMR spectral changes. The disappearance of the reactant **16** (5 mM) (δ 5.56 (OCHC), 6.85 and 8.03 (O₂NArH) for ¹H; δ -5.7 for ³¹P) matched the appearance of the product **17** (δ 5.09 (OCHC) for ¹H; δ 5.9 for ³¹P) and 4-nitrophenolate (δ 6.53 and 8.06) in D₂O at 35 °C and pD = 10.3 (0.1 M CHES buffer).

The hydrolysis rate (*v*₂) of the phosphodiester pendant in **16** was followed by UV spectroscopic measurement (at 400 nm) at pH 7.0–10.5 (20 mM Good's buffer), *I* = 0.10 (NaNO₃), and 35 °C. The first-order dependence on the total concentration of **16** (= [**16a**] + [**16b**] + [**16c**]) is consistent with the kinetic equation 9. The first-order rate constants *k'*_{PDE} are plotted as a function of pH in Figure 5. The sigmoidal curve indicates characteristic of a kinetic process controlled by an acid–base equilibrium and exhibits an inflection point at pH 9.0, which is almost the same as the p*K*_a value of 9.1 for the coordinate water of **16a**. Therefore, just as all the previous Zn^{II}-OH⁻ species,^{9d,10c} the Zn^{II}-OH⁻ in **16b** must be a good nucleophile to the intramolecular phosphate. The first-order rate constant *k*_{PDE} of (3.5 ± 0.1) × 10⁻⁵ s⁻¹ was obtained from the maximum *k'*_{PDE} (eq 10).

$$v_2 = k'_{\text{PDE}}[\text{total ZnL complex } \mathbf{16}] \quad (9)$$

$$= k_{\text{PDE}}[\mathbf{16b}] \quad (10)$$

A prolonged (ca. 1 week) alkaline reaction at 35 °C in 0.1 M aqueous NaOD solution did not change the ^{31}P NMR of **17** (δ 5.9), indicating that **17** is inert and undergoes no more hydrolysis. We assign the final product to the intramolecular phosphomonoester coordinating structure **17**. Earlier, we found that the Zn^{II} -cyclen complex **6a** tends to strongly bind to dianionic phosphomonoesters, e.g., $\log K = 3.3$ for 1:1 the NPP^{2-} - Zn^{II} -cyclen complex.¹⁴ Treatment of **17** (5 mM)²¹ with EDTA (25 mM) in D_2O at pD 10.3 (0.1 M CHES buffer) stripped Zn^{II} to free the ligand showing a singlet ^{31}P signal at δ 4.2.

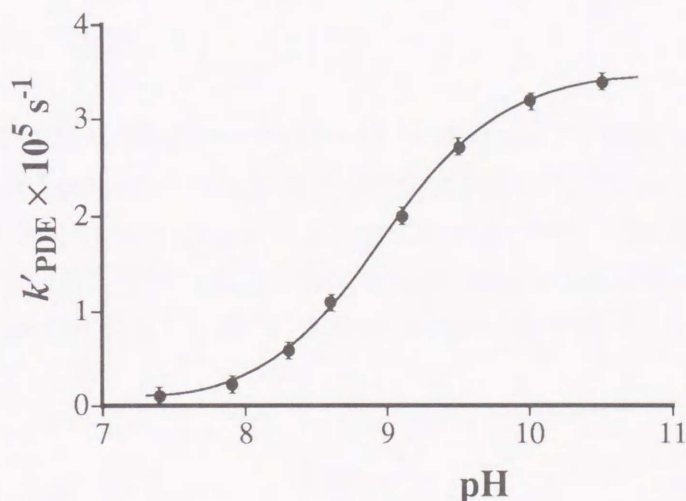


Figure 5. Rate-pH profile for the first-order rate constants of intramolecular phosphodiester hydrolysis of **16** (see eq 9) at 35 °C with $I = 0.10$ (NaNO_3) in aqueous solution.

3. Summary and Conclusions

The two-step mechanism of phosphate ester hydrolysis by Zn^{II}-containing alkaline phosphatase (AP) (Scheme 1) is well mimicked by the newly designed complex **14**: (i) a phosphoryl intermediate **16** is generated by attack of the hydroxy moiety of the alcohol pendant at the BNP⁻ (one of the ester group is concomitantly hydrolyzed) and (ii) the phosphoryl intermediate **16** is hydrolyzed by the intramolecular Zn^{II}-OH⁻. The attack at the BNP⁻ substrate and hydrolysis of the intermediate both require Zn^{II}. For the first step, the hydroxyl group is activated by Zn^{II} at physiological pH to **14b** (pK_a = 7.4), which is a 125 times more effective nucleophile to the phosphate substrate than the Zn^{II}-activated water of the reference **15b**. For the second step, the intramolecular nucleophile is generated from Zn^{II}-OH₂ **16a** with a pK_a value of 9. This intramolecular hydrolysis is 45 000 times faster than the intermolecular hydrolysis of NEP⁻ with 1 mM **15b**. In the AP enzyme (Scheme 1), these two functions of Zn^{II} are performed separately by two proximate Zn^{II} atoms; one is involved in the activation of Ser-102 to yield phosphoryl intermediate **2**, and the other is involved in the activation of H₂O **3** to attack at the intermediate **2**. The intramolecular arrangement of these two Zn^{II} ions in AP is more advantageous than our single-Zn^{II} system in order to provide this dual role, wherein the pK_a value of 9.0 (due to the close phosphate anion or the phosphate-binding) for **16a** ⇌ **16b** is higher than the reported pK_a value of 7.4 for **2** ⇌ **3** in the enzyme.

Scheme 4 summarizes the whole reaction mechanism of the P-O bond cleavage of the phosphodiester (BNP⁻) by **14**. The final phosphomonoester product **17**, unfortunately, was found to be very inert under normal conditions (all the attempts to hydrolyze it failed, including raising the pH as high as 11). Therefore, we could not use **14** as a catalyst. However, the present results may well serve the novel elucidation of the collaborative roles of Ser-102 and Zn^{II} in alkaline phosphatase.

4. Experimental Section

General Information. All reagents and solvents used were of analytical grade. The Good's buffers (Dojindo) were commercially available and used without further purification: MES (2-(*N*-morpholino)ethanesulfonic acid, $pK_a = 6.2$), MOPS (3-(*N*-morpholino)propanesulfonic acid, $pK_a = 7.2$), HEPES (*N*-(2-hydroxyethyl)piperazine-*N'*-2-ethanesulfonic acid, $pK_a = 7.6$), EPPS (*N*-(2-hydroxyethyl)piperazine-*N'*-3-propanesulfonic acid, $pK_a = 8.0$), TAPS (*N*-(tris(hydroxymethyl)methyl)amino-3-propanesulfonic acid, $pK_a = 8.4$), CHES (2-(cyclohexylamino)ethanesulfonic acid, $pK_a = 9.5$), CAPSO 3-(*N*-cyclohexylamino)-2-hydroxypropanesulfonic acid, $pK_a = 10.0$), CAPS 3-(*N*-cyclohexylamino)propanesulfonic acid, $pK_a = 10.4$). Sodium bis(4-nitrophenyl) phosphate was crystallized from an aqueous solution of bis(4-nitrophenyl) phosphoric acid (BNP) and equimolar NaOH. Lithium ethyl (4-nitrophenyl) phosphate was prepared by the reported method.²² DMF was distilled in vacuo over anhydrous $MgSO_4$ and stored in the dark. All aqueous solutions were prepared using deionized and distilled water.

Kinetic study was carried out using a Hitachi U-3500 spectrophotometer equipped with a thermoelectric cell temperature controller (± 0.5 °C). IR spectra were recorded on a Shimadzu FTIR-4200. 1H (400 MHz), ^{13}C (100 MHz), and ^{31}P (162 MHz) NMR spectra were recorded on a JEOL α -400 spectrometer. 3-(Trimethylsilyl)propionic-2,2,3,3- d_4 acid sodium salt (Aldrich) in D_2O and tetramethylsilane (Merck) in organic solvent were used as internal references for 1H and ^{13}C NMR measurements. A D_2O solution of 80% phosphoric acid was used as an external reference for ^{31}P NMR measurement. Optical rotations were recorded on a Union Giken Automatic Digital Polarimeter PM-101 at 22.0 ± 0.5 °C. Melting points were determined by using a Yanaco micro melting apparatus without any corrections. Elemental analysis was performed on a Yanaco CHN Corder MT-3. Thin layer (TLC) and silica gel column chromatographies were carried out on Merck Art. 5554 (silica gel) TLC plates and Wakogel C-300 (silica gel), respectively.

Synthesis of (*S*)-1-(2-Hydroxy-2-phenylethyl)-1,4,7,10-tetraazacyclododecane (11). 2,6-Dioxo-1,4,7,10-terazacyclododecane (**12**) (2.00 g, 10 mmol)¹⁶ and (*S*)-styrene oxide (1.32 g, 11 mmol) were heated to reflux in EtOH (100 mL) for 1 day. The reaction mixture was evaporated to dryness. The residue was purified by silica gel column chromatography (eluent $CH_2Cl_2/MeOH/28\%$ aqueous $NH_3 = 40:3:0.1$) followed by crystallization from CH_3CN to yield 1-(2-hydroxy-2-phenylethyl)-5,9-dioxo-1,4,7,10-tetraazacyclododecane (**13**) as colorless prisms (1.47 g, 4.6 mmol, 46% yield): mp 192.0–193.0 °C; IR (KBr pellet) 3362, 3086, 2975, 2955, 2822, 1655, 1539, 1455, 1435, 1348, 1316, 1291, 1269, 1227, 1200, 1169, 1071, 920, 870, 843, 774, 758, 706 cm^{-1} ; TLC (eluent $CH_2Cl_2/MeOH/28\%$ aqueous $NH_3 = 5:1:0.2$) $R_f = 0.4$; 1H NMR ($CDCl_3$) δ 1.83–2.06 (1H, br, amine NH), 2.51 (2H, dt, $J = 13.2, 4.6$ Hz, NCH), 2.64 (1H, dd, $J = 13.6, 4.0$ Hz, NCHAr), 2.77 (2H, ddd, $J = 13.2, 9.0, 4.2$ Hz, NCH), 2.84 (1H, dd, $J = 13.6, 9.4$ Hz, NCHAr), 3.16–3.24 (1H, br, alcohol OH; 2H, m, CONCH), 3.29 (1H, d, $J = 16.2$ Hz, CHCON),

3.34 (1H, d, $J = 16.2$ Hz, NCOCH), 3.44 (2H, m, CONCH), 4.79 (1H, dd, $J = 9.4, 4.0$ Hz, CHAr), 7.30 (1H, tt, $J = 6.4, 2.0$ Hz, ArH), 7.35 – 7.42 (4H, m, ArH), 7.43–7.48 (2H, br, amide NH); $[\alpha]_D -55.9^\circ$ (c 1.00, MeOH).

To a suspended solution of dioxo macrocycle **13** (1.92 g, 6.0 mmol) in dry THF (40 mL) was added slowly a THF solution (65 mL) of 1 M BH_3 -THF complex at 0°C . The mixture was stirred at room temperature for 1 h and then heated at 60°C for 1 day. After decomposition of the excess amount of the hydroborane complex with water at 0°C , the solvent was evaporated. The residue was dissolved in 6 M aqueous HCl (70 mL) and then the solution was heated at 70°C for 2 h. The mixture was washed with CH_2Cl_2 (30 mL \times 2) and evaporated to dryness. The residue was passed through an anion exchange column of Amberlite IRA-400 with water to obtain **11** as a colorless oil. Crystallization of the oil from 6 M aqueous HCl afforded colorless needles as its tetrahydrochloric acid salts (**11** \cdot 4HCl) in 62% yield (1.63 g, 3.7 mmol): dec 210°C ; IR (KBr pellet) 3420, 2998, 2793, 2448, 1576, 1495, 1439, 1066, 1028, 766, 704 cm^{-1} ; ^1H NMR (D_2O , pD 1.0) δ 2.82–3.21 (18H, m, NCH_2), 4.89 (1H, t, $J = 6.2$, OCHC), 7.40–7.54 (5H, m, ArH); ^{13}C NMR (D_2O , pD 1.0) δ 41.4, 41.5, 44.5, 44.6, 45.4, 47.0, 52.3, 52.4, 62.0, 73.8, 129.0, 131.5, 132.2, 144.8; $[\alpha]_D -49.1^\circ$ (c 1.00, H_2O). Anal. Calcd for $\text{C}_{16}\text{H}_{32}\text{N}_4\text{OCl}_4 \cdot \frac{1}{2}\text{H}_2\text{O}$: C, 43.0; H, 7.44; N, 12.5. Found: C, 43.1; H, 7.49; N, 12.4.

Synthesis of (*S*)-1-(2-Hydroxy-2-phenylethyl)-1,4,7,10-tetraazacyclododecane Zinc(II) Complex (14a** \cdot (ClO_4) $_2$).** **11** \cdot 4HCl (438 mg, 1.0 mmol) was passed through an anion exchange column of Amberlite IRA-400 with water to obtain the free ligand **11** as a colorless oil. After the oil was dissolved in water (4 mL), $\text{Zn}(\text{ClO}_4)_2 \cdot 6\text{H}_2\text{O}$ (391 mg, 1.1 mmol) was added in the solution. The solution was stirred at 60°C for 1 h. After the solvent was evaporated, the residue was recrystallized from water to obtain colorless prisms as diperchlorate salts **14a** \cdot (ClO_4) $_2$ in 91% yield (507 mg, 0.91 mmol): IR (KBr pellet) 3420, 3293, 2930, 2886, 1480, 1458, 1379, 1365, 1358, 1298, 1283, 1267, 1096, 968, 928, 860, 777, 756, 742, 708, 625 cm^{-1} ; ^1H NMR (D_2O , pD 6.0) δ 2.75–3.28 (18H, m, NCH), 5.14 (1H, dd, $J = 10.1, 3.2$ Hz, OCHC), 7.43–7.55 (5H, m, ArH); ^{13}C NMR (D_2O , pD 6.0) δ 45.97, 46.00, 46.2, 48.4, 48.5, 53.7, 55.0, 61.9, 72.4, 128.9, 131.4, 131.8, 144.0; $[\alpha]_D -64.4^\circ$ (c 1.00, H_2O). Anal. Calcd for $\text{C}_{16}\text{H}_{28}\text{N}_4\text{O}_9\text{Cl}_2\text{Zn}$: C, 34.5; H, 5.1; N, 10.1. Found: C, 34.7; H, 5.2; N, 10.0.

Preparation of Alkoxide Pendant Attached Zinc(II) Complex with **11 (**14b** \cdot ClO $_4$).** To a solution of **14a** \cdot (ClO_4) $_2$ (278 mg, 0.50 mmol) in MeOH (11 mL) was added 0.5 mL of 1 M methanolic NaOMe. Colorless solid was precipitated by slow evaporation and recrystallized from aqueous solution (pH 9.5) to obtain **14b** \cdot ClO $_4$ as colorless prisms in 96% yield (219 mg, 0.48 mmol): IR (KBr pellet) 3295, 2922, 2874, 1489, 1453, 1350, 1144, 1094, 982, 932, 855, 795, 774, 756, 710, 625 cm^{-1} ; ^1H NMR (D_2O , pD 9.5) δ 2.69–3.09 (17H, m, NCH_2),

3.22 (1H, ddd, $J = 13.8, 11.1, 4.3$ Hz, NCH_2), 4.86 (1H, t, $J = 6.6$ Hz, OCHC), 7.34–7.49 (5H, m, ArH); ^{13}C NMR (D_2O , pD 9.5) δ 45.2, 46.2, 46.6, 46.8, 47.6, 48.1, 52.6, 54.9, 63.5, 74.3, 129.2, 130.8, 131.6, 146.0; $[\alpha]_{\text{D}} -65.8^\circ$ (c 1.00, H_2O). Anal. Calcd for $\text{C}_{16}\text{H}_{27}\text{N}_4\text{O}_5\text{ClZn}$: C, 42.1; H, 6.0; N, 12.3. Found: C, 42.4; H, 6.0; N, 12.2.

Synthesis of (*S*)-1-(2-(4-Nitrophenylphosphoryl)-2-phenylethyl)-1,4,7,10-tetraazacyclododecane Zinc(II) Complex ($\mathbf{16a} \cdot \text{ClO}_4$). A DMF solution (8 mL) of $\mathbf{14b} \cdot \text{ClO}_4$ (91.3 mg, 0.20 mmol) and bis(4-nitrophenyl)phosphate sodium salt (72.4 mg, 0.20 mmol) was stirred at 35°C for 1 day. After the solvent was evaporated, the residue was dissolved in water (50 mL) and the pH was adjusted to 6.0 with 0.1 M aqueous HClO_4 . The aqueous solution was washed with diethyl ether (15 mL \times 3) and evaporated to dryness. The residue was recrystallized from water to obtain $\mathbf{16a} \cdot \text{ClO}_4$ as colorless prisms (98 mg, 0.15 mmol, 73% yield): dec 175°C ; IR (KBr pellet) 3303, 2934, 2885, 1611, 1591, 1514, 1493, 1458, 1346, 1252, 1146, 1090, 916, 864, 793, 754, 741, 700, 625, 550 cm^{-1} ; ^1H NMR (D_2O , pD 6.5) δ 2.93–3.30 (17H, m, NCH_2), 3.37 (1H, dd, $J = 15.3, 9.8$ Hz, NCH_2), 5.47 (1H, m, OCH), 7.02 (2H, dtd, $J = 9.3, 2.0, 0.9$ Hz, OArHNO_2), 7.33–7.46 (5H, m, CArH), 8.05 (2H, dtd, $J = 9.3, 2.0, 0.6$ Hz, OArHNO_2); ^{13}C NMR (D_2O , pD 6.5) δ 45.6, 45.7, 46.9, 47.0, 47.8, 47.9, 53.3, 56.7, 65.1 ($J_{\text{PC}} = 5.9$ Hz), 80.2 ($J_{\text{PC}} = 6.6$ Hz), 123.0 ($J_{\text{PC}} = 5.1$ Hz), 128.4, 129.1, 131.6, 131.7, 140.3, 146.5, 159.0 ($J_{\text{PC}} = 5.9$ Hz); ^{31}P NMR (D_2O , pD 6.5) δ -3.59 ($J_{\text{HP}} = 9.2, 2.7$ Hz); $[\alpha]_{\text{D}} -43.2^\circ$ (c 1.00, MeOH). Anal. Calcd for $\text{C}_{22}\text{H}_{33}\text{N}_5\text{O}_{11}\text{ClPZn}$: C, 39.1; H, 4.9; N, 10.4. Found: C, 38.9; H, 4.9; N, 10.4.

Syntheses of Racemic Ligand and its Zn^{II} Complexes. The racemic dioxocyclen derivative was prepared by the same method as that for $\mathbf{13}$ using *rac*-styrene oxide to give colorless prisms in 43% yield. Mp, TLC, IR, and NMR are the same as those for $\mathbf{13}$.

Using this dioxocyclen derivative, the racemic ligand (cyclen derivative) was prepared by the same method as $\mathbf{11}$ to give colorless needles as its tetrahydrochloric acid salts in 60% yield. Dec, IR, and NMR are the same as those for $\mathbf{11} \cdot 4\text{HCl}$. $[\alpha]_{\text{D}} = 0^\circ$ (c 1.00, H_3O). Anal. Calcd for $\text{C}_{16}\text{H}_{32}\text{N}_4\text{OCl}_4 \cdot \frac{1}{2}\text{H}_2\text{O}$: C, 43.0; H, 7.44; N, 12.5. Found: C, 43.0; H, 7.41; N, 12.1.

The pendant alcohol undissociated Zn^{II} complex with the racemic ligand was prepared by the same method as that for $\mathbf{14a}$ using the racemic ligand to give colorless prisms as its diperchlorate salts in 93% yield. IR and NMR are the same as those for $\mathbf{14a} \cdot (\text{ClO}_4)_2$. $[\alpha]_{\text{D}} = 0^\circ$ (c 1.00, H_2O). Anal. Calcd for $\text{C}_{16}\text{H}_{28}\text{N}_4\text{O}_9\text{Cl}_2\text{Zn}$: C, 34.5; H, 5.1; N, 10.1. Found: C, 34.8; H, 5.2; N, 10.1.

Using this Zn^{II} complex, the alkoxide pendant attached Zn^{II} complex was prepared with the same method as that for $\mathbf{14b}$ to give colorless prisms as perchlorate salts in 90% yield. IR and NMR are the same as those for $\mathbf{14b} \cdot \text{ClO}_4$. $[\alpha]_{\text{D}} = 0^\circ$ (c 1.00, H_2O). Anal. Calcd for $\text{C}_{16}\text{H}_{27}\text{N}_4\text{O}_5\text{ClZn}$: C, 42.1; H, 6.0; N, 12.3. Found: C, 42.0; H, 6.3; N, 12.3.

Crystallographic Study. A colorless prismatic crystal of **14b**·ClO₄ (0.40 × 0.40 × 0.20 mm) was used for data collection. The lattice parameters and intensity data were measured on a Rigaku AFC7R diffractometer with graphite monochromated Cu K α radiation and a 12-kW rotating anode generator. The structure was solved by a Patterson orientation/translation search and expanded using Fourier techniques. The non-hydrogen atoms were refined anisotropically. Hydrogen atoms were included but not refined. The final cycle of full-matrix least-squares refinement was based on 2862 observed reflections ($I > 3.00\sigma(I)$) to give $R = 0.050$ and $R_w = 0.077$. All calculations were performed using the teXsan crystal structure analysis package developed by Molecular Structure Corp. (1985 and 1992).

Potentiometric pH Titration. The preparation of the test solutions and the calibration method of the electrode system were described earlier.^{10,13} All test solutions (50 mL) were kept under an argon (>99.999% purity) atmosphere at 25.0 ± 0.1 °C with $I = 0.10$ (NaClO₄) and 35 ± 0.1 °C with $I = 0.10$ (NaNO₃). The potentiometric pH titrations were carried out at [total ligand] = 1 mM in the presence or absence of equimolar ZnSO₄, and [total Zn^{II} complex] = 1 mM, and at least three independent titration were made. The calculation methods for ligand protonation constants (K_n), Zn^{II} complexation constants ($K(\text{ZnL})$), and the deprotonation constant of the Zn^{II} complex (K_a) were the same as described previously.^{10,13} The protonation constants K_n are defined as $[\text{H}_n\text{L}]/[\text{H}_{n-1}\text{L}]a_{\text{H}^+}$, the 1:1 metal complexation constant $K(\text{ZnL})$ as $[\text{ZnL}]/[\text{Zn}^{\text{II}}][\text{L}]$, and the deprotonation constant K_a as $[\text{ZnH}_{-1}\text{L}]a_{\text{H}^+}/[\text{ZnL}]$. The used values of $K_w' (= [\text{H}^+][\text{OH}^-])$ and f_{H^+} were $10^{-13.79}$ and 0.825 at 25 °C, and $10^{-13.48}$ and 0.823 at 35 °C, respectively.

Kinetics Procedure for the Phosphodiester Cleavage Reaction with Zinc(II) Complexes in Aqueous Solution. The phosphodiester cleavage reaction (i.e., 4-nitrophenolate release reaction) rates of bis(4-nitrophenyl) phosphate (BNP⁻) and ethyl (4-nitrophenyl) phosphate (NEP⁻) were measured by an initial slope method (following the increase in 400-nm absorption of released 4-nitrophenolate) in aqueous solution at 35.0 ± 0.5 °C. Buffer solutions containing 20 mM Good's buffer (MES, pH 6.0; MOPS, pH 7.0; HEPES, pH 7.4; EPPS, pH 7.9; TAPS, pH 8.4; CHES, pH 9.3; CAPSO, pH 10.0) were used, and the ionic strength was adjusted to 0.10 with NaNO₃ (ca. 90 mM). For the initial rate determination, the following typical procedure was employed: BNP⁻ (10, 5.0, and 2.5 mM) and **14b** (2.0, 1.0, and 0.50 mM) were mixed in the buffered solution, the UV absorption increase recorded immediately and then followed generally until ca. 0.1% formation of 4-nitrophenolate, where log ϵ values for 4-nitrophenolate were 3.23 (pH 6.0), 3.94 (pH 7.0), 4.11 (pH 7.4), 4.20 (pH 7.9), 4.24 (pH 8.4), 4.26 (pH 9.3), and 4.26 (pH 10.0) at 400 nm. The observed first-order rate constant k_{obsd} (s⁻¹) was calculated from the decay slop (4-nitrophenolate release rate/[BNP⁻]). The value of $k_{\text{obsd}}/[\text{total Zn}^{\text{II}} \text{ complex}]$ gave the second-order rate constant k'_{BNP} (M⁻¹ s⁻¹) for BNP⁻ hydrolysis. The second-order rate constant k_{BNP} was

determined from the maximum k'_{BNP} values.

The second-order rate constants, k_{BNP} and k_{NEP} , for Zn^{II} -*N*-methylcyclen **15b** were determined by the same method for that for **14b** with BNP^- (10, 5.0, and 2.5 mM) and **15b** (16, 8.0, and 4.0 mM) and NEP^- (20, 10, and 5.0 mM) and **15b** (20, 10, and 5.0 mM), respectively.

Kinetics Procedure for the Phosphodiester Cleavage Reaction with **14b** in DMF.

The phosphodiester cleavage rate of bis(4-nitrophenyl) phosphate (BNP^-) was measured by an initial slope method (following the increase in 430-nm absorption of released 4-nitrophenolate) in DMF at 35.0 ± 0.5 °C. For the initial rate determination, the following procedure was employed. BNP^- (1.0, 0.50, and 0.25 mM) and **14b** (0.20, 0.10, and 0.050 mM) were mixed in DMF, the UV absorption increase recorded immediately and then followed generally until ca. 1% formation of 4-nitrophenolate, where $\log \epsilon$ of 4-nitrophenolate was 4.45 at 430 nm. The second-order rate constant k_{BNP} in DMF was determined by the similar method for k_{BNP} in aqueous solution.

Kinetics Procedure for Intramolecular Hydrolysis with 16b. The hydrolysis (i.e., 4-nitrophenolate release reaction) rate of **16b** was measured by an initial slope method (following the increase in 400-nm absorption of released 4-nitrophenolate) in aqueous solution at 35.0 ± 0.5 °C. Buffer solutions containing 20 mM Good's buffer (HEPES, pH 7.4; EPPS, pH 7.9; TAPS, pH 8.3 and 8.6; CHES, pH 9.1 and 9.5; CAPSO, pH 10.0; CAPS, pH 10.5) were used, and the ionic strength was adjusted to 0.10 with NaNO_3 (ca. 90 mM). For the initial rate determination, the following procedure was employed. **16b** (1.0, 0.50, and 0.25 mM) were mixed in the buffered solution, the UV absorption increase recorded immediately and then followed generally until ca. 1% formation of 4-nitrophenolate, where $\log \epsilon$ values for 4-nitrophenolate were 4.11 (pH 7.4), 4.24 (pH 8.3), 4.25 (pH 8.6), 4.26 (pH 9.1), 4.26 (pH 9.5), 4.26 (pH 10.0), and 4.27 (pH 10.5). The first-order rate constant k'_{PDE} (s^{-1}) was calculated from the decay slope. The first-order rate constant k_{PDE} (s^{-1}) was obtained from the maximum k'_{PDE} .

References and Notes

- (1) Coleman, J. E. *Annu. Rev. Biophys. Biomol. Struct.* **1992**, *21*, 441-483.
- (2) Kim, E. E.; Wyckoff, H. W. *J. Mol. Biol.* **1991**, *218*, 449-464.
- (3) (a) Gettins, P.; Coleman, J. E. *J. Biol. Chem.* **1984**, *259*, 4991-4997. (b) Hull, W. E.; Halford, S. E.; Gutfreund, H.; Sykes, B. D. *Biochemistry* **1976**, *15*, 1547-1561. (c) Bock, J. L.; Cohn, M. *J. Biol. Chem.* **1978**, *253*, 4082-4085. (d) Coleman, J. E.; Gettins, P. *Zinc Enzyme*; Birkhäuser: Boston, MA, 1986; Chapter 6, p 77.
- (4) For review; Fenton, D. E.; Okawa, H. *J. Chem. Soc., Dalton Trans.* **1993**, 1349-1357.
- (5) Ried, T. W.; Wilson, L. B. *Enzyme* **1971**, *4*, 373-415.
- (6) Butler-Ransohoff, J. E.; Rokita, S. E.; Kendall, D. A.; Banzon, J. A.; Carano, K. S.; Kaiser, E. T.; Matlin, A. R. *J. Org. Chem.* **1992**, *57*, 142-145.
- (7) (a) Mueller, E. G.; Crowder, M. W.; Averill, B. A.; Knowles, J. R. *J. Am. Chem. Soc.* **1993**, *115*, 2974-2975. (b) Coleman, J. E. *Zinc Enzyme*; Birkhäuser: Boston, MA, 1986; Chapter 4, p 49.
- (8) For a review of bimetallic enzyme models: (a) Göbel, M. W. *Angew. Chem., Int. Ed. Engl.* **1994**, *33*, 1141-1143. (b) Karlin, K. D. *Science* **1993**, *261*, 701-708.
- (9) (a) For Ir^{III} complexes: Hendry, P.; Sargeson, A. M. *J. Am. Chem. Soc.* **1989**, *111*, 2521-2527. (b) For Co^{III} complexes: Jones, D. R.; Lindoy L. F.; Sargeson, A. M. *J. Am. Chem. Soc.* **1983**, *105*, 7327-7336. Hendry, P.; Sargeson, A. M. *Inorg. Chem.* **1990**, *29*, 92-97. Chin, J.; Banaszczyk, M.; Jubian, V.; Zou, X. *J. Am. Chem. Soc.* **1989**, *111*, 186-190. Kim, J. H.; Chin, J. *J. Am. Chem. Soc.* **1992**, *114*, 9792-9795. Connolly, J. A.; Banaszczyk, M.; Hynes, R. C.; Chin, J. *Inorg. Chem.* **1994**, *33*, 665-669. (c) For Ln^{III} complexes: Schneider, H.-J.; Rammo, J.; Hettich, R. *Angew. Chem., Int. Ed. Engl.* **1993**, *32*, 1716-1719. Hay, R. W.; Govan, N. *J. Chem. Soc., Chem. Commun.* **1990**, 714-715. Morrow, J. R.; Buttrey, L. A.; Shelton, V. M.; Berback, K. A. *J. Am. Chem. Soc.* **1992**, *114*, 1903-1905. Chin, K. O. A.; Morrow, J. R. *Inorg. Chem.* **1994**, *33*, 5036-5041. Tsubouchi, A.; Bruice, T. C. *J. Am. Chem. Soc.* **1994**, *116*, 11614-11615. (d) For Zn^{II} complexes: Sigman, D. S.; Jorgensen, C. T. *J. Am. Chem. Soc.* **1972**, *94*, 1724-1731. Gellman, S. H.; Petter, R.; Breslow, R. *J. Am. Chem. Soc.* **1986**, *108*, 2388-2394. Hikichi, S.; Tanaka, M.; Moro-oka, Y.; Kitajima, N. *J. Chem. Soc., Chem. Commun.* **1992**, 814-815. Ruf, M.; Weis, K.; Vahrenkamp, H. *J. Chem. Soc., Chem. Commun.* **1994**, 135-136. (e) For Fe^{III} complexes: Wilkinson, E. C.; Dong, Y.; Que, L. Jr. *J. Am. Chem. Soc.* **1994**, *116*, 8394-8395.
- (10) (a) Kimura, E.; Shiota, T.; Koike, T.; Shiro, M.; Kodama, M. *J. Am. Chem. Soc.* **1990**, *112*, 5805-5811. (b) Kimura, E.; Koike, T.; Shionoya, M.; Shiro, M. *Chem. Lett.* **1992**, 787-790. (c) Koike, T.; Kimura, E. *J. Am. Chem. Soc.* **1991**, *113*, 8935-8941. (d) Zhang, X.; van Eldik, R.; Koike, T.; Kimura, E. *Inorg. Chem.* **1993**, *32*, 5749-5755. (e) Koike, T.; Kimura, E.; Nakamura, I.; Hashimoto, Y.; Shiro, M. *J. Am. Chem. Soc.* **1992**, *114*, 7338-7345.

- (f) Kimura, E.; Shionoya, M.; Hoshino, A.; Ikeda, T.; Yamada, Y. *J. Am. Chem. Soc.* **1992**, *114*, 10134-10137.
- (11) (a) Kimura, E.; Koike, T. *Comments Inorg. Chem.* **1991**, *11*, 285-301. (b) Kimura, E. In *Progress in Inorganic Chemistry*; Karlin, K. D., Ed.; John Wiley & Sons: New York, 1994; Vol. 41, 443-492.
- (12) Koike, T.; Takamura, M.; Kimura, E. *J. Am. Chem. Soc.* **1994**, *116*, 8443-8449.
- (13) Kimura, E.; Nakamura, I.; Koike, T.; Shionoya, M.; Kodama, Y.; Ikeda, T.; Shiro, M. *J. Am. Chem. Soc.* **1994**, *116*, 4764-4771.
- (14) Koike, T.; Kajitani, S.; Nakamura, I.; Kimura, E.; Shiro, M. *J. Am. Chem. Soc.* **1995**, *117*, 1210-1219.
- (15) The second-order rate constant for the 4-nitrophenolate release reaction from BNP^- with **8** (determined by initial slope method) is $(5.0 \pm 0.1) \times 10^{-4} \text{ M}^{-1} \text{ s}^{-1}$ in aqueous solution at 35 °C with $I = 0.10$ (NaNO_3). Kimura, E.; Koike, T. Unpublished results.
- (16) Kimura, E.; Kuramoto, Y.; Koike, T.; Fujioka, H.; Kodama, M. *J. Org. Chem.* **1990**, *55*, 42-46.
- (17) Shionoya, M.; Ikeda, T.; Kimura, E.; Shiro, M. *J. Am. Chem. Soc.* **1994**, *116*, 3848-3859. The Zn^{II} complexation constant $\log K(\text{ZnL})$ for **15a** is 15.1 ± 0.1 at 25 °C with $I = 0.10$ (NaClO_4). Kimura, E.; Ikeda, T. Unpublished results.
- (18) Kimura, E.; Koike, T.; Toriumi, K. *Inorg. Chem.* **1988**, *27*, 3687-3688.
- (19) Hence, the $\text{p}K_{\text{a}}$ was determined using the titration data before 0.5% hydrolysis of pendant phosphate.
- (20) (a) A second-order rate constant for hydrolysis of 4-nitrophenyl acetate with **14b** in DMF ($(1.1 \pm 0.1) \times 10^2 \text{ M}^{-1} \text{ s}^{-1}$ at 35 °C) is also 350 times greater than the rate in aqueous solution ($0.31 \pm 0.01 \text{ M}^{-1} \text{ s}^{-1}$ at 35 °C with $I = 0.10$ (NaNO_3)). Kimura, E.; Kodama, Y. Unpublished results. (b) We have given a thought to running the hydrolysis with $\text{Zn}^{\text{II}}\text{-OH}^-$ complex **15b** in dry DMF as a reference reaction. However, we could not isolate **15b** in any of the attempts using various counteranions such as ClO_4^- , PF_6^- , Cl^- , etc. Generation of **15b** in situ makes the reaction more complex and difficult to interpret.
- (21) The solution of **17** was prepared by the reaction of **16a** (5 mM) in D_2O at 50 °C and pD 10.3 (0.1 M CHES buffer) for 1 day.
- (22) (a) Morrow, J. R.; Trogler, W. C. *Inorg. Chem.* **1988**, *27*, 3387-3394. (b) Kirby, A. J.; Younas, M. *J. Chem. Soc. B* **1970**, 1165-1172.

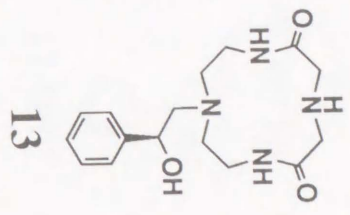
謝辞

本研究を行うにあたり、終始御指導、御鞭撻を賜りました 広島大学医学部総合薬学科教授 木村榮一先生に心より謹んで感謝の意を表わします。

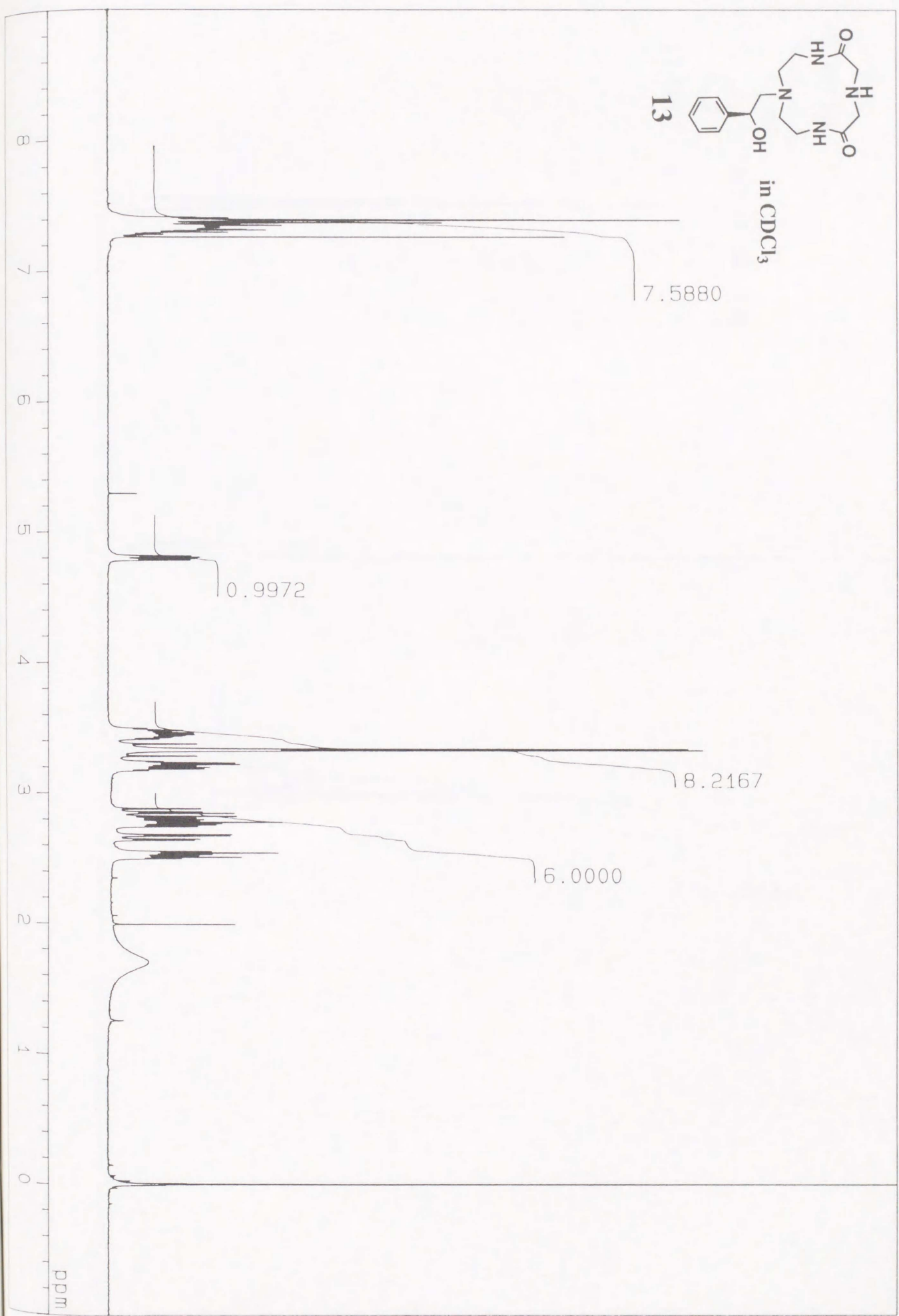
研究のみならず公私共に御指導、御鞭撻を賜りました 広島大学医学部総合薬学科助教授 小池透先生、本学科助手 青木伸先生、現国立分子科学研究所教授 塩谷光彦先生、現つくば工業技術院 高橋利和先生、ならびに木村研究室の皆様および卒業された先輩方に心より御礼申し上げます。

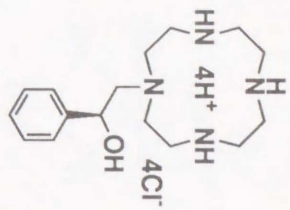
X線結晶構造解析を行っていただきました、理学電機株式会社 城始勇先生に深謝致します。

平成7年12月 児玉頼光



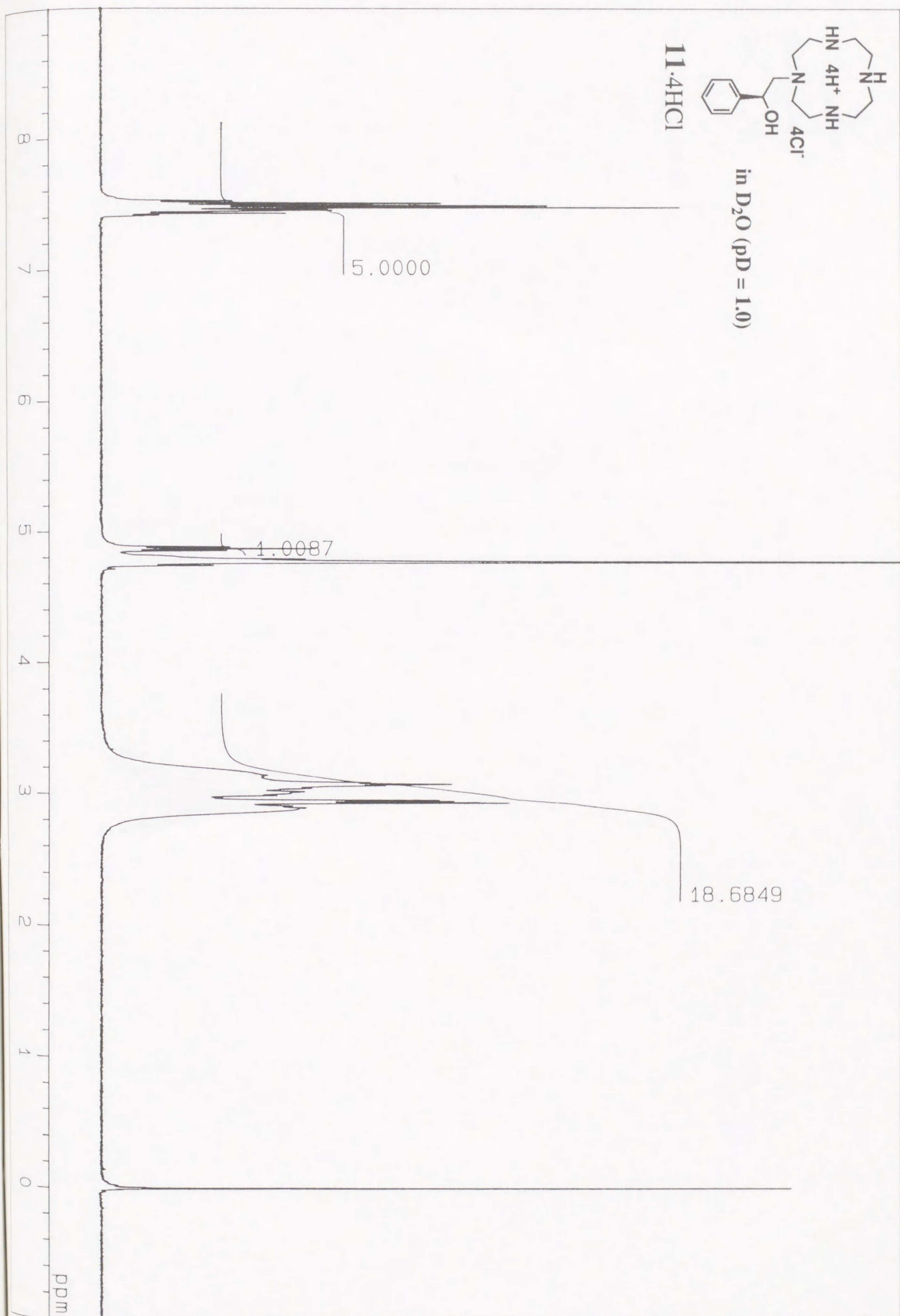
in CDCl₃

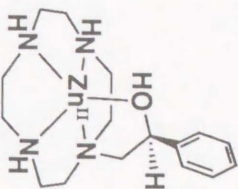




11·4HCl

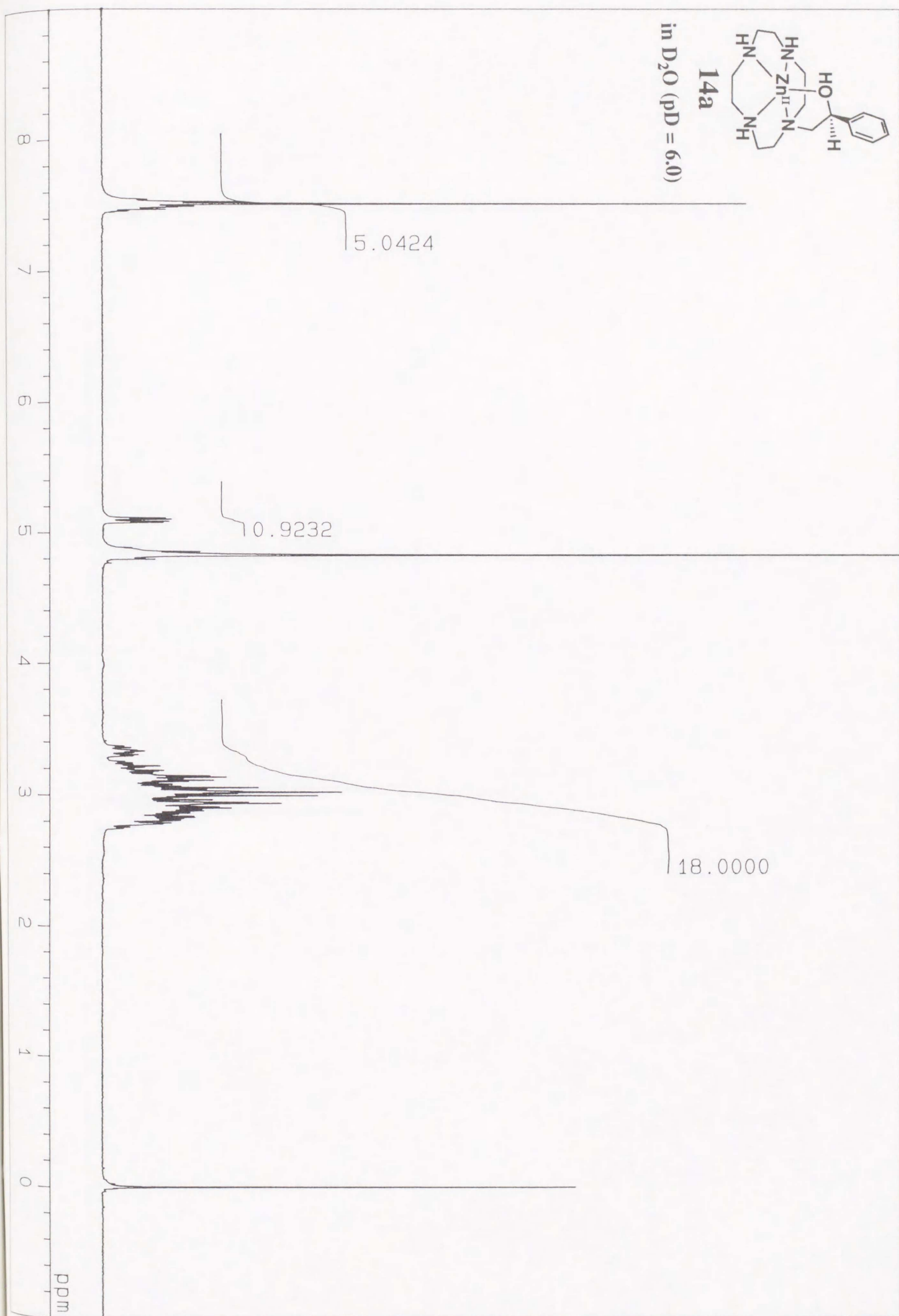
in D₂O (pD = 1.0)

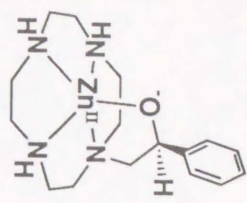




14a

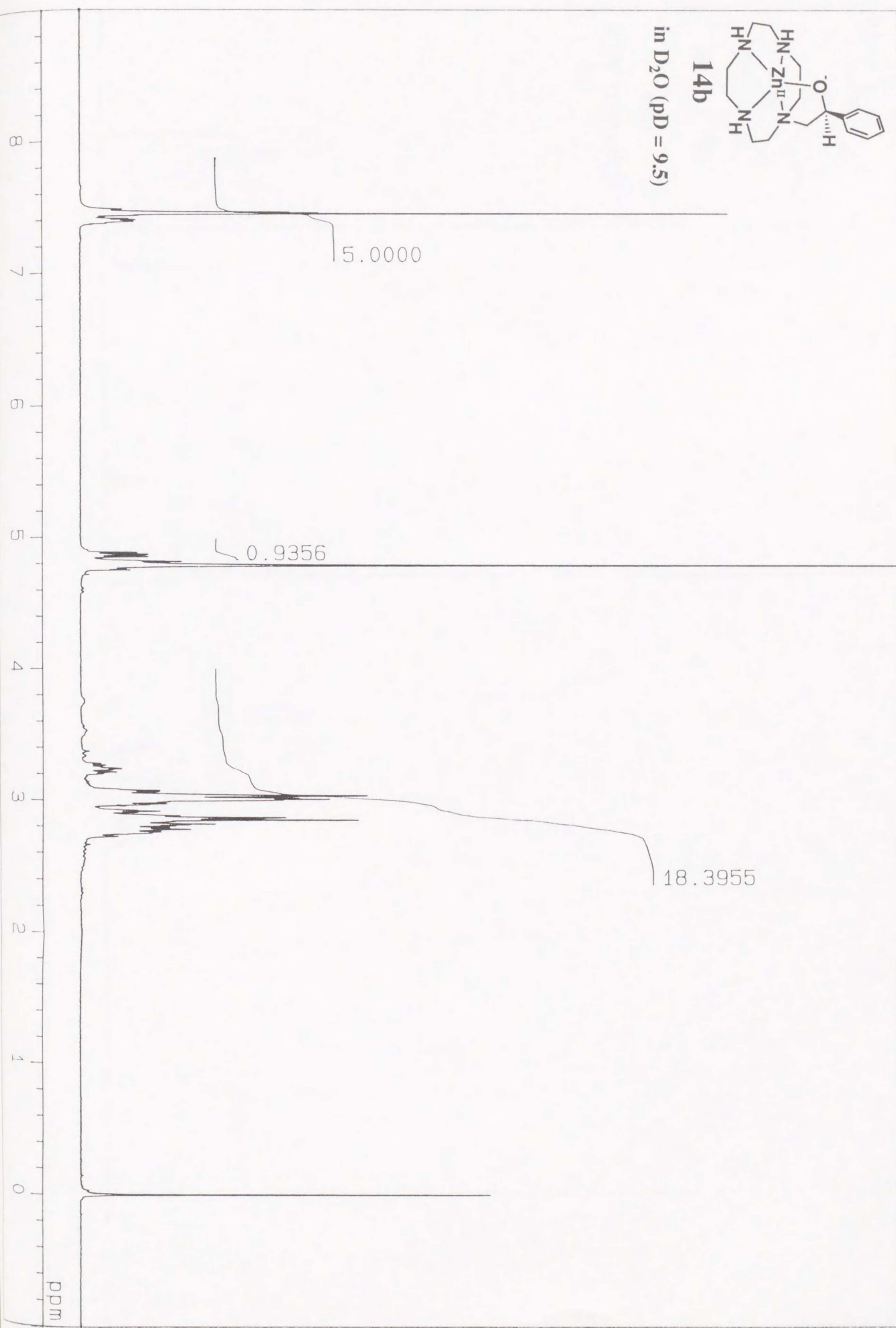
in D₂O (pD = 6.0)

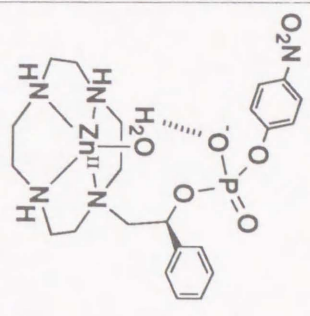




14b

in D₂O (pD = 9.5)





16a

in D₂O (pD = 6.5)

